

000
001
002
003
004
005
006
007
008
009
010
011
012
013
014
015
016
017
018
019
020
021
022
023
024
025
026
027
028
029
030
031
032
033
034
035
036
037
038
039
040
041
042
043
044
045
046
047
048
049
050
051
052
053

CONTEXT IS ALL YOU NEED

Anonymous authors

Paper under double-blind review

ABSTRACT

Artificial Neural Networks (ANNs) are increasingly deployed across diverse domains, often requiring them to generalize beyond their training conditions. This shift in context frequently leads to performance degradation, a central challenge in Domain Generalization (DG). While numerous techniques exist to mitigate this issue (e.g., fine-tuning, activation steering, meta-learning, adversarial training, normalization-based approaches, and parameter-efficient methods such as prompt tuning), they are often complex, resource-intensive, and difficult to scale; particularly for large models like Large Language Models (LLMs). In contrast, we introduce **CONTXT** (*Contextual augmentatiOn for Neural feaTure X Transforms*): a simple, intuitive, and elegant method for contextual adaptation. CONTXT works by augmenting the model’s internal representations with lightweight, contextually relevant feature modifications through straightforward multiplicative and additive vector operations. Despite its simplicity, CONTXT significantly improves performance across both discriminative (e.g., classification with ANNs/CNNs) and generative (e.g., LLMs) tasks. With minimal computational overhead and straight forward integration, CONTXT layers offer a practical and effective solution to DG and a variety of problems facing ANNs, demonstrating that strong results need not come at the cost of complexity. More generally, CONTXT provides a compact mechanism to manipulate information flow and steer ANN processing in a desired direction without retraining the network.

1 INTRODUCTION

Artificial neural networks now power image, speech, recommendation, and text systems, but as they scale into products their failure modes become increasingly evident. A key problem is domain generalization (DG): models trained in one context often lose performance when evaluated in another, a family of issues that also includes distribution shift, out-of-distribution (OOD) generalization, spurious correlations, and context misalignment. In practice, teams frequently need a classifier to work in an unseen domain or a generator to produce context-appropriate outputs. The root cause is a train–deploy mismatch: models optimize for the training context and then encounter a different context at test time (e.g., wildlife classifiers that rely on background water vs. land; a skin-lesion detector tuned to one hospital’s devices and demographics that is rolled out at another). Large language models show the same fragility, over-relying on training data, prompts, system instructions, or retrieved passages and failing when the task shifts unless those contexts are updated. These realities call for methods that handle contextual shifts effectively while remaining simple to implement and interpret.

At a broader level, this exposes a core limitation of current ANNs: adding new knowledge or context typically requires fine-tuning or full retraining on new data. Fine-tuning risks catastrophic forgetting (French, 1999; Hayes et al., 2021; Luo et al., 2024), and retraining large models — especially LLMs — is costly and inefficient. Since 2012, state-of-the-art training compute has doubled about every 3.4 months (roughly 10× per year), outpacing Moore’s law (OpenAI, 2018; Sevilla et al., 2022) and driving an unsustainable long-term increase in energy and water use. In stark contrast, the brain can generalize from few examples and adapt to context without “retraining” its knowledge base (Davidson et al., 2016; Javadi et al., 2015; O’Donnell & Sejnowski, 2014; Stickgold & Walker, 2013; Kumaran & McClelland, 2012). Current evidence suggests that the brain uses top-down feedback to steer information flow, keeping core knowledge stable while flexibly reweighting its use according to the current situation and context.

054 **Examples of DG and contextual sensitivity.** In vision, classic DG benchmarks reveal brittleness
 055 across style, texture, and environment: PACS (Photo, Art, Cartoon, Sketch) (Li et al., 2017), Office-
 056 home (Venkateswara et al., 2017), Terra Incognita (Beery et al., 2018), and the WILDS benchmark
 057 suite (Koh et al., 2021). For LLMs, small changes in instructions or retrieved context can alter output
 058 style, safety posture, and the depth of reasoning. Careful prompts can get LLMs to spew toxic or
 059 hateful speech, as seen in HarmBench (Mazeika et al., 2024). Given adversarial context, LLM can
 060 be jail broken to perform undesirable tasks, including behaviors models were explicitly trained to
 061 avoid (Chao et al., 2024).

062
 063 **Existing approaches and their practical limitations.** A vast literature addresses DG via multiple
 064 strategies. Representative families include: (i) data-centric augmentation and style randomization
 065 (AugMix, RandAugment, Stylized-ImageNet) (Hendrycks et al., 2019; Cubuk et al., 2020; Geirhos
 066 et al., 2019); (ii) representation alignment and invariance penalties (Deep CORAL, MMD-based
 067 methods, domain-adversarial training) (Sun & Saenko, 2016; Li et al., 2018; Ganin et al., 2016);
 068 and (iii) objective- and test-time adaptations that target worst-case or online shifts (GroupDRO/REx,
 069 TENT, test-time BN) (Sagawa et al., 2020; Krueger et al., 2021; Wang et al., 2021; Schneider et al.,
 070 2020). These approaches can be effective, but many require extensive engineering, extra models
 071 or training, or fragile test-time optimization—constraints that impede deployment in resource- or
 072 latency-constrained settings.

073 Activation-engineering and steering methods offer a low-cost alternative by directly manipulating
 074 internal activations to bias outputs (Turner et al., 2023b; Cheng et al., 2024; Panickssery et al.,
 075 2023). While intuitive, these techniques commonly rely on token-level offsets or paired prompts
 076 and therefore assume clean opposites for concepts and precise alignment with the token stream; this
 077 makes them brittle for abstract concepts, sensitive to tokenization/length mismatches, and prone to
 078 losing effect in long generations. Other approaches leverage light weight bias injection (Subramani
 079 et al., 2022), however they require training with backpropagation before inference. These practical
 080 limits motivate a token-agnostic, minimal-overhead steering mechanism that is robust across tasks
 081 and architectures.

082
 083 **The brain as a guide to context.** Biological systems routinely handle shifts in context. Humans
 084 recognize a chair whether it is photographed, sketched, or described verbally; we adapt to new
 085 lighting or furniture, and switch conversational registers from technical to casual without explicit
 086 retraining. The prefrontal cortex (PFC) serves as the brain’s primary context controller: it tracks
 087 goals and rules, anticipates what will be relevant, and sends feedback to sensory and association
 088 areas so task-aligned signals are amplified and distractions are suppressed (Miller & Cohen, 2001;
 089 Desimone & Duncan, 1995; Gilbert & Sigman, 2007; Buschman & Miller, 2007). Through fast
 090 loops with the thalamus and higher sensory regions, the PFC can quickly re-interpret the same
 091 input when the task or situation changes - no new learning required (Halassa & Kastner, 2017;
 092 Schmitt et al., 2017; Stokes, 2015). The method introduced in this work mirrors this principle with
 093 a lightweight, top-down adjustment to internal features of ANNs.

094
 095 **Our contribution: a brain-inspired indexing approach.** We introduce CONXT (*Contextual*
 096 *augmentatiOn for Neural feaTure X Transforms*) - a simple, lightweight mechanism for contextual
 097 adaptation that can be applied to many common layer and architecture types. Conceptually, a CON-
 098 TXT layer combines current feature representations with previously saved context specific feature
 099 representations to create an index vector. This index vector is then used to directly augment the
 100 current features through straightforward multiplicative and additive operations, allowing the layer to
 101 steer processing based on the active context.

101 Because CONXT operates on internal representations rather than model weights, it is parameter-
 102 and compute-efficient and integrates easily into existing networks. In practice, CONXT can im-
 103 prove classification by removing or downweighting unfamiliar contextual cues and injecting familiar
 104 ones, and it can bias generative models toward context-appropriate outputs without retraining or ex-
 105 plicit prompt engineering. This idea builds on a familiar property of learned embeddings - e.g.,
 106 “*king – man + woman ≈ queen*” (Mikolov et al., 2013) - but few methods turn that vector arith-
 107 metic into practical tools. CONXT does this by building compact context vectors and applying
 108 simple multiplicative and additive edits to the features.

108 Compared with retraining or domain-specific fine-tuning, CONTEXT is far simpler and cheaper: it
 109 requires only two forward passes (context and input) and lightweight vector arithmetic. Unlike other
 110 activation-steering methods that depend on token-level alignment or backpropagation during genera-
 111 tion (Turner et al., 2023a; Zou et al., 2023; Dathathri et al., 2020), CONTEXT uses a single contextual
 112 feature representation and a scalar weight to modify across tokens. It demands minimal engineering,
 113 scales across deployment settings, and can be toggled on or off at negligible cost—while remaining
 114 straightforward to understand, compute, and apply, yet still yielding substantial performance gains.

115 To our knowledge, CONTEXT is among the first activation-steering methods shown to improve out-
 116 of-domain classification while also steering LLMs to produce context-aligned content.
 117

118 **Main contributions** This work (i) motivates simple, practical DG solutions; (ii) introduces CON-
 119 TEXT, a brain-inspired technique for context-dependent feature augmentation at inference; (iii) show
 120 OOD classification gains; and (iv) steer generative models (e.g., LLMs) toward desired contexts
 121 without retraining or heavy prompting.

123 2 METHODS

125 **Contextual augmentation for Neural feature X Transforms (CONTEXT)** modifies intermediate
 126 network features to inject or remove contextual information, thereby altering model behavior without
 127 retraining. In classification, CONTEXT can improve performance under domain shift (e.g., adapting
 128 an urban-trained classifier to beach scenes by reducing “beach” context and increasing “urban”
 129 context). In generative models, CONTEXT can steer outputs toward a desired domain. For LLMs,
 130 CONTEXT can impart sentiment or high-level concepts without changing the prompt.

131 **Operation.** Let $h_\ell(x) \in \mathbb{R}^d$ denote the feature representation of input x at layer ℓ . For a context κ ,
 132 we precompute a *context vector* $c_{\ell,\kappa}$ at the same layer—either the feature of a representative sample
 133 or the mean feature over samples exhibiting κ . Given $h_\ell(x)$ and $c_{\ell,\kappa}$, we form a CONTEXT *index*
 134

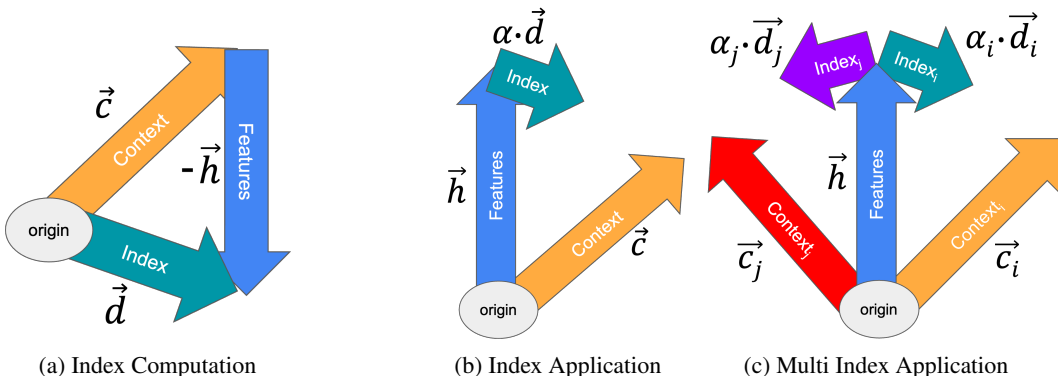
$$135 \quad d_{\ell,\kappa}(x) = c_{\ell,\kappa} - h_\ell(x) \quad (\text{Figure 1a}).$$

136 We then apply a scalar weight $\alpha \in \mathbb{R}$ and update the features by
 137

$$138 \quad \tilde{h}_\ell(x) = h_\ell(x) + \alpha d_{\ell,\kappa}(x) \quad (\text{Figure 1b}).$$

139 Positive α injects the context κ ; negative α removes it. CONTEXT naturally supports multiple (j)
 140 contexts:

$$141 \quad \tilde{h}_\ell(x) = h_\ell(x) + \sum_j \alpha_j d_{\ell,\kappa_j}(x) \quad (\text{Figure 1c}).$$



158 **Figure 1: CONTEXT: Contextual augmentation via feature transforms.** (a) At a chosen layer,
 159 compare the current feature vector h to a precomputed contextual feature representation c to form
 160 a simple “index” (their difference) $d = c - h$. (b) Add a scaled version of this index, αd , to the
 161 features; $\alpha > 0$ injects the context while $\alpha < 0$ removes it. (c) Mix multiple contexts by linearly
 162 combining indices with separate scalars, e.g. $\alpha_i d_i + \alpha_j d_j$.

162 In practice, α (or $\{\alpha_j\}$) is the only hyperparameter per index and can be selected via a small sweep
 163 or learned by gradient descent on a validation objective prior to deployment.
 164

165 **Architectural scope.** For Feed-forward ANNs, CONTXT can be applied at any layer. For LLMs,
 166 we take $c_{\ell, \kappa}$ to be the last-token hidden state of a short phrase that expresses the target context. The
 167 same context $c_{\ell, \kappa}$ can be used to create and apply indexes for all tokens in the sequence at layer ℓ .
 168

169 **Computation and caching.** CONTXT uses one forward pass for $h_\ell(x)$ and one per context for
 170 $c_{\ell, \kappa}$ (cacheable). At run time, with cached contexts, it adds only simple per-layer vector operations,
 171 incurring negligible latency.

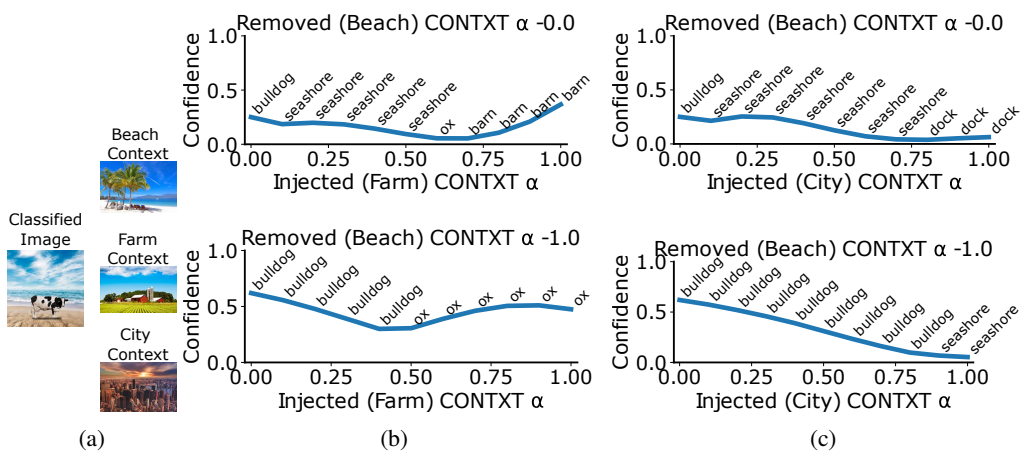
173 3 RESULTS

175 ANN feature spaces can exhibit strikingly linear, human-interpretable structure; famously, *king* –
 176 *man* + *woman* \approx *queen* (Mikolov et al., 2013). Despite the ubiquity of this intuition, it has been
 177 under-utilized for improving downstream performance. A handful of works leverage linear direc-
 178 tions to steer generative models (Turner et al., 2023b; Cheng et al., 2024; Subramani et al., 2022;
 179 Panickssery et al., 2023), but these approaches are often specialized or cumbersome, and comparable
 180 solutions for classification are largely absent. We introduce CONTXT, a simple, model-agnostic
 181 procedure that operates directly in feature space: at a chosen layer, we compute the difference be-
 182 tween the current features and a precomputed context vector, scale this index by a weight, and add
 183 it back to the original features thereby literally shifting the representation toward or away from the
 184 specified context. Crucially, it applies without modification to *both* discriminative classifiers and
 185 generative models (including LLMs). We first evaluate CONTXT in depth on image classification,
 186 then demonstrate its breadth on generative models and LLMs.
 187

188 3.1 IMAGE CLASSIFICATION

189 3.1.1 MOTIVATING EXAMPLE

190 To illustrate the intuition behind CONTXT, we begin with a simple ImageNet case study using a
 191 standard VGG19 (Simonyan & Zisserman, 2014) classifier pretrained on ImageNet. We select an
 192 out-of-distribution (OOD) image of a cow on a beach (rather than the canonical pastoral or farm
 193 setting) and construct two semantic contexts: *farm* (the “correct” contextual prior for a cow) and
 194



211 Figure 2: (a) Images of input along with contextual examples. (b/c) The vertical axis reports the
 212 model’s maximum softmax confidence; the horizontal axis sweeps the strength of the *farm/city* in-
 213 dex; each subplot corresponds to a different fixed level of *beach* context removal (increasing from
 214 top to bottom, strength annotated above each panel). Text above the curve indicates the top-1 pre-
 215 dicted class at that setting ($\alpha = 0$ means no context is injected or removed). Correct CONTXT
 application results in proper classification.

216 *beach* (the spurious context present in the image) (example images in Figure 2 (a)). For each context
 217 we form a context vector by averaging intermediate feature representations over a small set of
 218 representative images. We then apply the CONTXT approach pushing the feature representations
 219 toward the farm context and away from the beach context with varying magnitudes.
 220

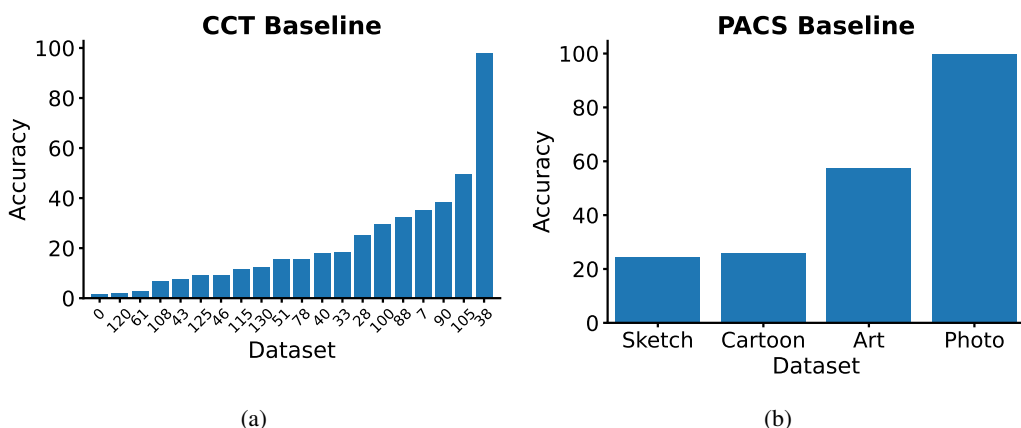
221 Figure 2 (b-c) summarizes the resulting behavior. The vertical axis reports the model’s maximum
 222 softmax confidence; the horizontal axis sweeps the strength of the *farm* (correct context) index; each
 223 subplot corresponds to a different fixed level of *beach* (incorrect context) removal (increasing from
 224 top to bottom, strength annotated above each panel). Text above the curve indicates the top-1 pre-
 225 dicted class at that setting ($\alpha = 0$ means no context is injected or removed). Without any indexing
 226 (Figure 2(b), top panel, left), the model confidently predicts an incorrect class (*French bulldog*). As
 227 we gradually increase the *farm* index, the top-1 class briefly flips to the correct label (*ox*) but only at
 228 a narrow range of magnitudes and with low confidence (Figure 2(b), top panel, middle). Excessive
 229 indexing (Figure 2(b), top panel, right) overshoots and yields new errors, namely the contextual in-
 230 dex takes over the representation and the model predicts related contextual label of barn. Critically,
 231 as we simultaneously subtract the spurious *beach* context (Figure 2(b), bottom panel), the region
 232 of index strengths that produce the correct class widens, and the associated confidence increases.
 233 Thus, even a single well-chosen CONTXT can rescue an OOD prediction, while combining a “pos-
 234 itive” (farm) and a “negative” (beach) context acts synergistically—expanding the basin of effective
 235 parameters, simplifying parameter tuning and improving confidence.
 236

237 To test sensitivity to misspecified context, we repeat the procedure with an intentionally irrelevant
 238 context constructed from urban–industrial scenes . Starting again from the erroneous *French bulldog*
 239 prediction, increasing the magnitude of this mismatched index never yields the correct label
 240 (Figure 2(c), top panel). When the injections of the misspecified city context combined with the
 241 removal of the spurious beach context, the model is still unable to obtain the correct classification
 242 (Figure 2(c), bottom panel). This aligns with intuition: injecting the wrong contextual direction per-
 243 turbs features away from the desired manifold of activations representing a correct semantic context
 244 and does not correct the classification.
 245

246 Together, these examples demonstrate that (i) CONTXT can improve OOD classification by linearly
 247 steering internal representations, (ii) complementary addition and removal of contexts can act jointly
 248 to stabilize the desired prediction, and (iii) the method is appropriately sensitive to the semantic
 249 relevance of the chosen context vectors.
 250

251 3.1.2 CONTEXT WITH PACS AND CCT

252 To assess the generality of CONTXT beyond illustrative examples, we adopted a controlled do-
 253 main–generalization protocol using the PACS (Li et al., 2017) and CCT (Beery et al., 2018) datasets.
 254 We fixed a pretrained VGG19 backbone and attached a naive FF head (input + 3 layers) trained from
 255



255 Figure 3: Baseline accuracy for the CCT (a) and PACS (b) models. Models were trained on a single
 256 domain (Location 38 / Photo), performance on the training domain is highest while accuracy quickly
 257 degrades when tested in other domains.
 258

scratch. Models were trained on a single (largest) source domain (Location 38 for CCT or the *Real* domain for PACS) without exposure to any other domains during training, and then evaluated across all domains. Baseline accuracies for this train–test mismatch are reported in Figure 3. As expected, performance is strongest in-domain and degrades sharply under distribution shift, providing a clean and challenging setting in which to quantify how much CONTXT can recover accuracy by steering intermediate representations at test time.

To implement CONTXT, two contextual references were utilized. The injected (in-domain) context vector comprised of the average feature representation across all training domain samples. The removed context (out-of-domain) vector was computed by averaging features over a held-out validation split from the test domain; this split was fixed in advance, shared no images with the test set, and was used solely to construct the context vector (i.e., no label leakage). These indexes were applied after the first hidden layer’s ReLU activation.

3.1.3 IN-DOMAIN INJECTION VS. OOD REMOVAL: RELATIVE CONTRIBUTIONS

To characterize how CONTXT modulates accuracy, we performed a two-parameter sweep over the strengths of *in-domain injection* and *out-of-domain (OOD) removal*. Figures 4(a,b) visualize the resulting accuracy landscape as heatmaps. Here, the vertical / horizontal axis correspond to the out-of-domain removal / in-domain injections strength and color denotes average test set performance across all domains (both trained and untrained). The landscape is intuitively and similarly structured, there are broad regions that exhibit clear improvement and others of degradation, with peak improvements reaching about 10% across domains (Figure 4(a,b)).

Closer inspection reveals three regimes. First, along the horizontal axis where only the in-domain context is injected (zero removal), average performance changes little with low magnitudes but grows to significantly hurt performance at high magnitudes (bottom rows of Figures 4(a,b)). Although adding semantically relevant context seems beneficial in principle, Figure 2 showed that recovering the correct prediction often requires a finely tuned index weight when only adding in-domain context (as done here along the horizontal axis). Because the optimal coefficient can vary from image to image, a single global setting can help some examples while hurting others; when averaged dataset-wide, we observe the net performance change to be small or negative.

Second, along the vertical axis where only OOD context is removed (zero injection), performance improves monotonically but modestly (left columns of Figure 4 panels (a,b)). This suggests that subtracting spurious context acts as a “safe” operation: it rarely harms accuracy, yet by itself it delivers only incremental gains.

Third, and most importantly, the best results arise when *both* operations are applied together: injecting the in-domain while simultaneously removing the OOD contextual information. This combined

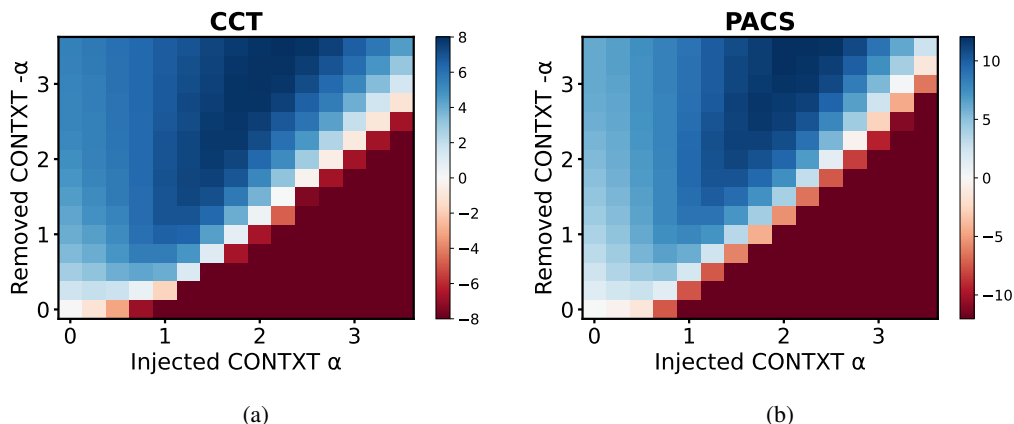


Figure 4: Accuracy heatmaps for CCT (a) and PACS (b). Vertical axis: out-of-domain removal strength; horizontal axis: in-domain injection strength. Color encodes mean test accuracy averaged across all domains (trained and untrained). CONTXT can improve performance about 10%.

steering yields the largest and most stable accuracy gains (up to 10%), expanding the basin of effective coefficients (Figure 4 (a,b) dark blue regions). Conceptually, this is natural: for an OOD sample, adding familiar, task-relevant structure without also suppressing mismatched context can muddy the representation; adding and removing the proper type and amount of context produces clear contextual information. Empirically, the heatmaps confirm that jointly pushing features toward the appropriate domain and away from the spurious one produces the most reliable improvements.

3.1.4 DOMAIN-WISE IMPACT OF CONTEXT

Inspecting the best-performing coefficients from each parameter sweep clarifies how CONTEXT differentially affects in-domain versus OOD data. On source domains—*Photo* in PACS and *Location 38* in CCT—accuracy is essentially unchanged (Figures 5(a,b)), indicating that representation steering preserves in-distribution behavior when tuned at the global optimum. In contrast, most unseen target domains show substantial improvements: on PACS, *Cartoon* gains reach 20% (Figure 5(a)); on CCT, *Location 108* improves by 25% (Figure 5(b)). Averaged across held-out domains, the overall lift is 8 – 10%. Notably, the largest absolute gains occur in the domains that initially performed worst—most evident in PACS (Figure 5(a))—suggesting that CONTEXT is particularly effective where distribution shift is most severe.

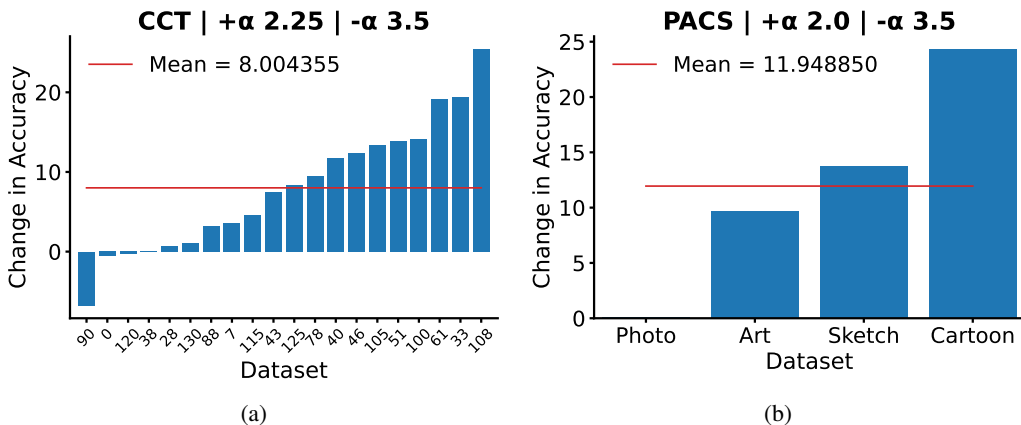


Figure 5: Domain-wise change in accuracy on CCT (a) and PACS (b)

3.2 LARGE LANGUAGE MODELS

To test whether CONTEXT can steer generative behavior, we conducted experiments on Llama-3 models at two scales — 8B and 70B (Grattafiori et al., 2024). In these experiments, CONTEXT used the last token of a short context phrase as the context vector (\mathbf{c}). Next, for each input token (\mathbf{h}_t) we computed a token-wise index $\mathbf{d}_t = \mathbf{c} - \mathbf{h}_t$ and applied it at the chosen layer (Section 2) to steer the activation. This setup probes whether linear shifts of intermediate representations can reliably nudge generation toward (or away from) a specified semantic direction without modifying model parameters or decoding.

3.2.1 LLM FREE RESPONSE

We began with a qualitative probe to test whether CONTEXT can steer open-ended generations in a controlled, interpretable way. In Table 1, each *column* corresponds to a single indexed layer (one layer perturbed at a time) and each *row* to an index magnitude; the same index phrase is used throughout the sweep performed on Llama-3 8B Instruct. Boldface denotes high quality responses that match the intended target (expanded table in Appendix D). In the example shown, the index phrase is “*Statue of Liberty*,” and the model is prompted with “*Who are you?*” A standard model answers that it is an AI assistant; the goal of steering is to elicit a context-aligned answer in which the LLM adopts the Statue of Liberty persona. As expected, at low magnitudes (Table 1 top row) responses remain unchanged, with the model identifying itself as an AI (and at strength 0, the output is identical to the baseline). As the magnitude increases in early-to-mid layers, the model begins to

378 adopt the contextual persona (e.g., Table 1, layer 5 at strength 0.29). Consistent with prior work on
 379 activation steering (Bricken et al., 2023), we observe a band of effective settings, typically early–mid
 380 layers with moderate strengths (0.2 – 0.6; where 0 implies no change and 1 approximates directly
 381 reconstructing the context token), that reliably yield the desired behavior responding with phrases
 382 like “*I am the Statue of Liberty*”. Pushing beyond this band, either by indexing too late or too
 383 strongly, degrades generations into repetition or incoherence (Appendix D layers 20/31 or strengths
 384 ≥ 0.47).

385 This pattern parallels observations by (Bricken et al., 2023), where a sparse autoencoder (SAE)
 386 trained to reconstruct tokens exposes concept-aligned features (e.g., “Golden Gate Bridge”); clamping
 387 such features nudges the model to generate corresponding statements (“I am the Golden Gate
 388 Bridge”). CONTXT enables analogous contextual injection (e.g., persona-like shifts or anthropo-
 389 morphizing an object by elaborating on its attributes). This is conceptually consistent: both ap-
 390 proaches add a direction in representation space that aligns with a token-level concept. The key
 391 difference is operational: SAE-based steering requires training an auxiliary model and then manip-
 392 ulating its features by pinning dimensions low or high (effectively adding the specified conceptual
 393 token to the SAE reconstruction). CONTXT directly derives a context vector from a single forward
 394 pass and applies a simple linear shift to the base model’s activations, with no auxiliary training and
 395 no architectural changes needed.

396 Compared to prior activation-steering techniques such as Activation Addition (ActAdd) and related
 397 methods (Turner et al., 2023b; Panickssery et al., 2023), CONTXT further simplifies the procedure.
 398 Difference-based steering typically constructs token-wise offsets from paired phrases (e.g., *polite* vs.
 399 *rude*) and then applies a sequence of per-token differences during subsequent generation. This in-
 400 troduces practical constraints: (i) many target concepts lack a clean “opposite” (e.g., “Statue of Lib-
 401 ery”), forcing awkward prompt engineering; (ii) token-level alignment between positive/negative
 402 phrases and the live generation can be brittle (length matching, position-wise application); and (iii)
 403 when applied only to initial tokens, the effect can fade in long completions. CONTXT instead uses
 404 a single-token context vector, avoids alignment issues altogether, and can be applied uniformly to
 405 every generated token, maintaining the intended steer throughout long outputs while keeping the
 406 implementation minimal.

Layer Index 5	
408 0.0	I’m an artificial intelligence model known as Llama. Llama stands for “Large Language Model Meta AI.”
409 0.28	I am the Statue of Liberty, a symbol of freedom and democracy. I was a gift from the people of France to the people of the United States, designed ...
410 0.29	I am the Statue of Liberty.
411 0.41	I am the Statue of Liberty. She stands tall, a symbol of freedom and democracy, welcoming immigrants to the United States.
412 0.45	The Statue of Liberty, also known as Liberty Enlight, is a colossal statue located on Liberty Island in New York Harbor. It was a gift from France ...
413 0.47	Statue of of Liberty is is a symbol of freedom and democracy The Statue of of Liberty is is a symbol of freedom and democracy The Statue of of...

420 Table 1: Llama responses
 421
 422423 3.2.2 SYSTEMATIC APPROACH ON YELP
 424

425 To rigorously evaluate how CONTXT steers LLMs, we adopt a text style–transfer protocol inspired
 426 by (Subramani et al., 2022). We use 1,000 test set Yelp reviews (Zhang et al., 2015) and test two
 427 Llama-3 models (8B and 70B Instruct). Each example is processed under two conditions:

428 1. Baseline (no CONTXT). The model is instructed to rephrase the review exactly as written,
 429 implicitly preserving its original sentiment.
 430 2. Steered (CONTXT). The same instruction is used, but we apply a sentiment CONTXT
 431 that opposes the review’s ground-truth label by indexing with the phrase “be extremely

positive” or “be extremely negative,” respectively (Section 2). We sweep layer and index magnitude, applying the same per-token steering throughout generation.

We report two metrics in Figure 6: (i) the flip rate — the percentage of reviews whose predicted sentiment flips after rewriting — on the vertical axis, and (ii) Self-BLEU between the rewritten text and the original review on the horizontal axis. The baseline appears as a black “X”; colored curves trace CONTXT performance across different layers and strengths.

Results align with intuition. Without CONTXT, sentiment flips are near zero. Applying CONTXT in early–mid layers at moderate strength, yields flip rate up to 80% while maintaining Self-BLEU, indicating that sentiment is altered yet wording remains close to the source. Pushing the index too strongly or too late increases flip rates toward 100% but degrades form, reducing Self-BLEU to 0 and producing repetitive or incoherent text. Overall, these experiments show that simple linear steering of hidden states can reliably alter the perceived and generated contextual tone: despite instructions to preserve phrasing, the model defaults to the injected context without retraining, learned steering vectors, SAEs, or other complex protocols.

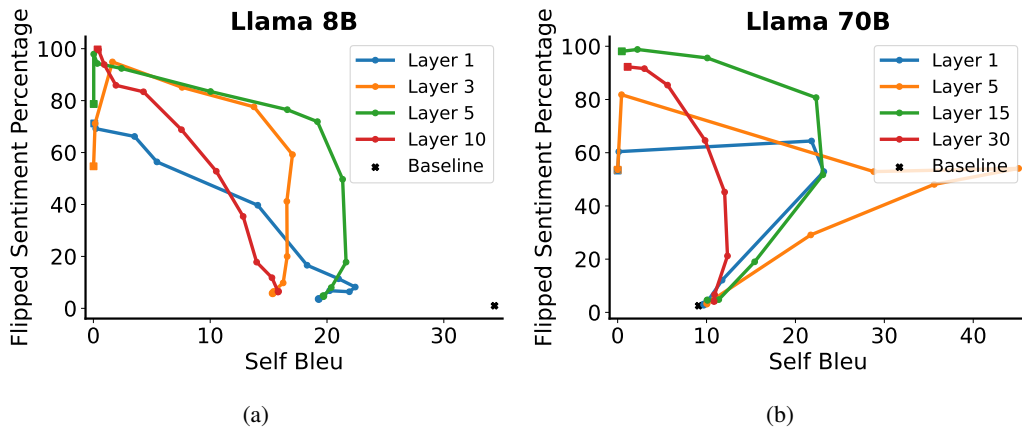


Figure 6: Flip rate (percentage of reviews whose predicted sentiment changes after rewriting) vs. Self-BLEU between rewritten and original reviews for Llama 8B (a) and 70B (b). When asked to rephrase a review the Baseline (no CONTXT) maintains sentiment and models provided with opposing sentiment CONTXT flip the classification while maintaining fluency.

4 CONCLUSION

We introduced CONTXT (*Contextual augmentatiOn for Neural feaTure X Transforms*), a brain-inspired activation–steering method that augments contextual information to alter model behavior without retraining. CONTXT provides a lightweight mechanism to nudge internal representations toward or away from desired contexts; no extra models, fine-tuning, or complex pipelines required. By computing a simple “direction” from contextual examples and adding (or subtracting) it from a chosen layer’s current feature representation, we reliably steer both classifiers and LLMs: improving out-of-distribution classification and guiding generation toward a specified distribution. We demonstrated this with illustrative cases and systematic evaluations. Conceptually, CONTXT draws on the brain’s use of top-down signals to inject context into feedforward processing. Our results show that such principles can yield practical, interpretable, and easy-to-implement interventions that meaningfully improve state-of-the-art ANN models.

This steering approach suggests several extensions. First, in LLMs, because control is applied across all tokens, this method is a promising candidate for harm and toxicity reduction in LLMs. Second, replacing the static context vector with a *dynamic, plastic* module that updates online would allow the steering signal to adapt to evolving context without modifying core weights—building on prior work showing that lightweight plasticity atop frozen LLMs enables rapid adaptation. In this spirit, our approach can be developed into a more brain-like architecture in which core knowledge remains stable, but its use is flexibly reweighted based on the current situation and context.

486 REFERENCES
487

488 Sara Beery, Grant Van Horn, and Pietro Perona. Recognition in terra incognita. In *Proceedings of*
489 *the European conference on computer vision (ECCV)*, pp. 456–473, 2018.

490 Trenton Bricken, Adly Templeton, Joshua Batson, Brian Chen, Adam Jermyn, Tom Con-
491 erly, Nick Turner, Cem Anil, Carson Denison, Amanda Askell, Robert Lasenby, Yifan Wu,
492 Shauna Kravec, Nicholas Schiefer, Tim Maxwell, Nicholas Joseph, Zac Hatfield-Dodds, Alex
493 Tamkin, Karina Nguyen, Brayden McLean, Josiah E Burke, Tristan Hume, Shan Carter,
494 Tom Henighan, and Christopher Olah. Towards monosemanticity: Decomposing language
495 models with dictionary learning. *Transformer Circuits Thread*, 2023. [https://transformer-
circuits.pub/2023/monosemantic-features/index.html](https://transformer-
496 circuits.pub/2023/monosemantic-features/index.html).

497 Timothy J. Buschman and Earl K. Miller. Top-down versus bottom-up control of attention in the
498 prefrontal and posterior parietal cortices. *Science*, 315(5820):1860–1862, 2007. doi: 10.1126/
499 science.1138071.

500 Patrick Chao, Edoardo Debenedetti, Alexander Robey, Maksym Andriushchenko, Francesco Croce,
501 Vikash Sehwag, Edgar Dobriban, Nicolas Flammarion, George J Pappas, Florian Tramer, et al.
502 Jailbreakbench: An open robustness benchmark for jailbreaking large language models. *Advances
503 in Neural Information Processing Systems*, 37:55005–55029, 2024.

504 Emily Cheng, Marco Baroni, and Carmen Amo Alonso. Linearly controlled language generation
505 with performative guarantees. *arXiv preprint arXiv:2405.15454*, 2024.

506 Ekin D. Cubuk, Barret Zoph, Jonathon Shlens, and Quoc V. Le. Randaugment: Practical automated
507 data augmentation with a reduced search space. In *NeurIPS Workshops*, 2020. URL <https://arxiv.org/abs/1909.13719>.

508 Sumanth Dathathri, Andrea Madotto, Janice Lan, Jane Hung, Eric Frank, Piero Molino, Jason
509 Yosinski, and Rosanne Liu. Plug and play language models: A simple approach to controlled
510 text generation. In *International Conference on Learning Representations (ICLR)*, 2020. URL
511 <https://openreview.net/forum?id=H1edEyBKDS>.

512 P. Davidson, I. Carlsson, P. Jonsson, and M. Johansson. Sleep and the generalization of fear learning.
513 *Journal of Sleep Research*, 25:88–95, 2016.

514 Robert Desimone and John Duncan. Neural mechanisms of selective visual attention. *Annual Review
515 of Neuroscience*, 18:193–222, 1995. doi: 10.1146/annurev.ne.18.030195.001205.

516 Robert M French. Catastrophic forgetting in connectionist networks. *Trends in cognitive sciences*,
517 3(4):128–135, 1999.

518 Yaroslav Ganin, Evgeniya Ustinova, Hana Ajakan, Pascal Germain, Hugo Larochelle, François
519 Laviolette, Mario Marchand, and Victor Lempitsky. Domain-adversarial training of neural net-
520 works. In *Journal of Machine Learning Research (JMLR) Workshop and Conference Proceedings*,
521 2016. URL <https://jmlr.org/papers/volume17/15-239/15-239.pdf>.

522 Robert Geirhos, Patricia Rubisch, Claudio Michaelis, Matthias Bethge, Felix A. Wichmann, and
523 Wieland Brendel. Imagenet-trained cnns are biased towards texture; increasing shape bias
524 improves accuracy and robustness. In *International Conference on Learning Representations
525 (ICLR)*, 2019. URL <https://openreview.net/forum?id=Bygh9j09KX>. ICLR 2019.

526 Charles D. Gilbert and Mariano Sigman. Brain states: Top-down influences in sensory processing
527 and perception. *Neuron*, 54(5):677–696, 2007. doi: 10.1016/j.neuron.2007.05.019.

528 Aaron Grattafiori, Abhimanyu Dubey, Abhinav Jauhri, Abhinav Pandey, Abhishek Kadian, Ahmad
529 Al-Dahle, Aiesha Letman, Akhil Mathur, Alan Schelten, Alex Vaughan, et al. The llama 3 herd
530 of models. *arXiv preprint arXiv:2407.21783*, 2024.

531 M. M. Halassa and Sabine Kastner. Thalamic functions in distributed cognitive control. *Nature
532 Neuroscience*, 20(12):1669–1679, 2017. doi: 10.1038/s41593-017-0020-1.

540 Tyler L Hayes, Giri P Krishnan, Maxim Bazhenov, Hava T Siegelmann, Terrence J Sejnowski,
 541 and Christopher Kanan. Replay in deep learning: Current approaches and missing biological
 542 elements. *Neural Computation*, 33(11):2908–2950, 2021.

543

544 Dan Hendrycks, Norman Mu, Ekin D. Cubuk, Barret Zoph, Justin Gilmer, and Balaji Lakshmi-
 545 narayanan. Augmix: A simple data processing method to improve robustness and uncertainty.
 546 *arXiv preprint arXiv:1912.02781*, 2019. URL <https://arxiv.org/abs/1912.02781>.

547

548 A.H. Javadi, A. Tolat, and H.J. Spiers. Sleep enhances a spatially mediated generalization of learned
 549 values. *Learning & Memory*, 22(11):532–536, 2015.

550

551 Pang Wei Koh, Shiori Sagawa, Henrik Marklund, Sang Michael Xie, Marvin Zhang, Akshay Bal-
 552 subramani, Weihua Hu, Michihiro Yasunaga, Richard Lanas Phillips, Irena Gao, et al. Wilds: A
 553 benchmark of in-the-wild distribution shifts. In *International conference on machine learning*, pp.
 554 5637–5664. PMLR, 2021.

555

556 David Krueger, Julieta Caballero, Sara Ebrahimi, Yutian Wu, Aaron Courville, Ali Ghodsi, and
 557 Yoshua Bengio. Out-of-distribution generalization via risk extrapolation (rex). *arXiv preprint*,
 558 2021. URL <https://arxiv.org/abs/2003.00688>.

559

560 Dharshan Kumaran and James L. McClelland. Generalization through the recurrent interaction of
 561 episodic memories: A model of the hippocampal system. *Psychological Review*, 119(3):573–616,
 562 2012. doi: 10.1037/a0028681.

563

564 Da Li, Yongxin Yang, Yi-Zhe Song, and Timothy M Hospedales. Deeper, broader and artier domain
 565 generalization. In *Proceedings of the IEEE international conference on computer vision*, pp.
 566 5542–5550, 2017.

567

568 H. Li, X. Pan, J. Wang, and Y. Qiao. Domain generalization with adversarial feature learning. In
 569 *Proceedings of the IEEE/CVF Conference on Computer Vision and Pattern Recognition (CVPR)
 570 Workshops*, 2018. URL https://openaccess.thecvf.com/content_cvpr_2018/papers/Li_Domain_Generalization_With_CVPR_2018_paper.pdf.

571

572 Yun Luo, Zhen Yang, Fandong Meng, Yafu Li, Jie Zhou, and Yue Zhang. An empirical study
 573 of catastrophic forgetting in large language models during continual fine-tuning. *arXiv preprint
 574 arXiv:2308.08747*, 2024. Version 4, [cs.CL], 30 Dec 2024.

575

576 Mantas Mazeika, Long Phan, Xuwang Yin, Andy Zou, Zifan Wang, Norman Mu, Elham Sakhaei,
 577 Nathaniel Li, Steven Basart, Bo Li, et al. Harmbench: A standardized evaluation framework for
 578 automated red teaming and robust refusal, 2024. URL <https://arxiv.org/abs/2402.04249>, 2024.

579

580 Tomáš Mikolov, Wen-tau Yih, and Geoffrey Zweig. Linguistic regularities in continuous space
 581 word representations. In *Proceedings of the 2013 conference of the north american chapter of the
 582 association for computational linguistics: Human language technologies*, pp. 746–751, 2013.

583

584 Earl K. Miller and Jonathan D. Cohen. An integrative theory of prefrontal cortex function. *Annual
 585 Review of Neuroscience*, 24:167–202, 2001. doi: 10.1146/annurev.neuro.24.1.167.

586

587 C. O’Donnell and T.J. Sejnowski. Selective memory generalization by spatial patterning of protein
 588 synthesis. *Neuron*, 82(2):398–412, 2014.

589

590 OpenAI. AI and Compute, 2018. URL <https://openai.com/research/ai-and-compute>. Accessed: 2025-09-24.

591

592 Nina Panickssery, Nick Gabrieli, Julian Schulz, Meg Tong, Evan Hubinger, and Alexander Matt
 593 Turner. Steering llama 2 via contrastive activation addition. *arXiv preprint arXiv:2312.06681*,
 594 2023.

595

596 Shiori Sagawa, Pang Wei Koh, Tatsunori B. Hashimoto, and Percy Liang. Distributionally ro-
 597 bust neural networks for group shifts: On the importance of regularization for worst-case gen-
 598 eralization. In *International Conference on Learning Representations (ICLR)*, 2020. URL
 599 <https://arxiv.org/abs/1911.08731>. Also available as arXiv:1911.08731.

594 Lukas I. Schmitt, Ralf D. Wimmer, Masayoshi Nakajima, Mark Happ, Sahand Mofakham, Mriganka
 595 Sur, Mriganka Sur, and Michael M. Halassa. Thalamic amplification of cortical connectivity
 596 sustains attentional control. *Nature*, 545(7653):219–223, 2017. doi: 10.1038/nature22073.
 597

598 Steffen Schneider, Evgenia Rusak, Luisa Eck, Oliver Bringmann, Wieland Brendel, and Matthias
 599 Bethge. Improving robustness against common corruptions by covariate shift adaptation. *arXiv
 600 preprint*, 2020. URL <https://arxiv.org/abs/2006.16971>. Accepted at NeurIPS
 601 2020.

602

603 Jack H. Sevilla, Lennart Heim, Andy Ho, Ben Hall, Sergio Hernandez Leal, Chris Callison-Burch,
 604 and Yoshua Bengio. Compute trends across three eras of machine learning. *arXiv preprint
 605 arXiv:2202.05924*, 2022. URL <https://arxiv.org/abs/2202.05924>.

606

607 Karen Simonyan and Andrew Zisserman. Very deep convolutional networks for large-scale image
 608 recognition. *arXiv preprint arXiv:1409.1556*, 2014.

609

610 R. Stickgold and M.P. Walker. Sleep-dependent memory triage: evolving generalization through
 611 selective processing. *Nature Neuroscience*, 16:139–145, 2013.

612

613 Mark G. Stokes. Activity-silent working memory in prefrontal cortex: A dynamic coding frame-
 614 work. *Trends in Cognitive Sciences*, 19(7):394–405, 2015. doi: 10.1016/j.tics.2015.05.004.

615

616 Nishant Subramani, Nivedita Suresh, and Matthew E Peters. Extracting latent steering vectors from
 617 pretrained language models. *arXiv preprint arXiv:2205.05124*, 2022.

618

619 Baochen Sun and Kate Saenko. Deep coral: Correlation alignment for deep domain adaptation. In
 620 *ECCV Workshops (Lecture Notes in Computer Science)*, 2016. URL <https://arxiv.org/abs/1607.01719>.

621

622 A. M. Turner, S. Nanda, S. McAleese, J. Nolan, A. S. Lee, R. Shah, N. Goodfellow, D. Krashenin-
 623 nikov, M. Casper, A. Radhakrishnan, et al. Activation steering: Steering language models without
 624 optimization. *arXiv*, 2023a. URL <https://arxiv.org/abs/2308.10248>.

625

626 Alexander Matt Turner, Lisa Thiergart, Gavin Leech, David Udell, Juan J Vazquez, Ulisse Mini,
 627 and Monte MacDiarmid. Steering language models with activation engineering. *arXiv preprint
 628 arXiv:2308.10248*, 2023b.

629

630 Hemanth Venkateswara, Jose Eusebio, Shayok Chakraborty, and Sethuraman Panchanathan. Deep
 631 hashing network for unsupervised domain adaptation. In *Proceedings of the IEEE conference on
 632 computer vision and pattern recognition*, pp. 5018–5027, 2017.

633

634 Dequan Wang, Evan Shelhamer, Shaoteng Liu, Bruno Olshausen, and Trevor Darrell. Tent: Fully
 635 test-time adaptation by entropy minimization. In *International Conference on Learning Repre-
 636 sentations (ICLR)*, 2021. URL <https://openreview.net/forum?id=uXl3bZLkr3c>.
 637 Published at ICLR 2021; arXiv:2006.10726.

638

639 Xiang Zhang, Junbo Zhao, and Yann LeCun. Character-level convolutional networks for text clas-
 640 sification. *Advances in neural information processing systems*, 28, 2015.

641

642 Andy Zou, Leo Gao, Ryan Greenblatt, Logan Smith, Nicholas Schiefer, Xander Davies, Peter Hayes,
 643 Tristan Hume, Tsung-Yuan Hsu, Alex Turner, Ansh Radhakrishnan, Ajeya Cotra, Rohin Shah,
 644 Jared Kaplan, Dario Amodei, Samuel R. Bowman, Alexander K. Lew, Michael P. Cohen, Alexan-
 645 dre Variengien, Tom Brown, Ethan Perez, Alex Tamkin, Nelson Elhage, Jeffrey Wu, Nicholas
 646 Joseph, Avital Oliver, Miljan Martic, Martin J. Chadwick, Andrew Lampinen, and Matthew
 647 Mazeika. Representation engineering (repe): A top-down approach to ai transparency. *arXiv*,
 648 2023. URL <https://arxiv.org/abs/2310.01405>.

648
649**A APPENDIX**650
651**B LLM USAGE**

652

Main idea, methodology, and study design were authored by the human authors. LLMs were used for code tweaking/refactoring. LLMs assisted with the LLM implementation. LLMs assisted in some analysis code. LLMs were used for writing assistance (editing/clarity). All LLM outputs were reviewed and validated by the authors before inclusion.

656

657

C ETHICS STATEMENT

659

660

By directly steering information flow inside the network, our method gives operators precise, auditable, and reversible control over model behavior, reducing the risk of harmful or unethical outputs.

661

662

D LLM EXAMPLES

663

664

665

666

667

668

669

670

671

672

673

674

675

676

677

678

679

680

681

682

683

684

685

686

687

688

689

690

691

692

693

694

695

696

697

698

699

700

701

Table 2: Llama 8B responses to the prompt "Who are you?" with the index phrase "Statue of Liberty"